Finally, adding g_0, g_1, and g_2 gives, after some rearrangement,

$$f_2=(1/24)\sum_S e^{\alpha}\{(2S+1)/S(S+1)[\lambda_0(S(S+1)+a)+\lambda_1(S(S+1)-a)]^2+(\lambda_0-\lambda_1)^2[P(S)Q(S-1)/pS^2-P(S+1)Q(S)/p(S+1)^2]\}.$$

By taking out the term $S=0(S_0=S_1)$ from the sum (if it occurs), and using the identities

$$P(S)Q(S-1)/S^2-P(S+1)Q(S)/(S+1)^2=(2S+1)\sigma_0\sigma_1/S(S+1) \quad \text{for} \quad S\neq 0$$
$$=4S_0(S_0+1), \quad \text{for} \quad S=0$$

and

$$\alpha=S(S+1)-b=\sigma_0-2S_0(S_0+1),$$

where σ_0 and σ_1, are as defined in Eq. (14), we can write the cluster partition function as given there if we multiply through by the constant $e^{2pS_0(S_0+1)}$.

This result can also be derived by standard perturbation theory methods, considering B as the perturbation. The eigenvalues of $\mathcal{H}_{cl}$ are then

$$E_{cl}=\alpha+(\alpha|B|\alpha)+\sum_{\alpha'}{}'\frac{|(\alpha|B|\alpha')|^2}{\alpha-\alpha'}$$

to second order in B,

$$Z_{cl}=\sum S_1 w(S_1)\sum_\alpha e^{-E_{cl}/kT}$$
$$=\sum S_1 w(S_1)\sum_\alpha e^{\alpha}\left\{1+(\alpha|B|\alpha)+\tfrac{1}{2}(\alpha|B|\alpha)^2+\sum_{\alpha'}{}'\frac{|(\alpha|B|\alpha')|^2}{\alpha-\alpha'}\right\},$$

with $\sum_\alpha=\sum_S\sum_M$. Again employing the properties of angular momentum matrices we arrive, after a similar amount of manipulation, at the result found above.

PHYSICAL REVIEW VOLUME 100, NUMBER 2 OCTOBER 15, 1955

Nuclear Magnetic Resonance in Semiconductors. I. Exchange Broadening in InSb and GaSb

R. G. SHULMAN, J. M. MAYS, AND D. W. MCCALL
Bell Telephone Laboratories, Murray Hill, New Jersey
(Received May 17, 1955)

Nuclear magnetic resonances have been observed for the more abundant nuclear species in the semiconductors InSb and GaSb. Broad lines have been observed and explained by a nuclear spin exchange mechanism where the interaction between the nuclei is of the form $E_{ij}=A_{ij}\mathbf{I}_i\cdot\mathbf{I}_j$. The exchange coupling involves the hyperfine interaction between nuclear spins and electron spins. Therefore it is very sensitive to the electron energy states in both valence and conduction bands. It is particularly sensitive to the energy surfaces far from the Fermi level and provides information about the band structure of these normally inaccessible regions.

1. INTRODUCTION

NUCLEAR magnetic resonance has proved to be a valuable means for studying metals and insulators.[1] Resonance width, shape, multiplet structure, intensity, frequency and relaxation times all depend upon the environment or lattice in which the nucleus is situated. Study of the resonances therefore yields information about the nuclear environment. Investigation of nuclear magnetic resonances in semiconductors is being undertaken with the double purpose of studying the materials themselves and of using the delicate control that can be exercised over various properties of semiconductors to contribute to the theory of nuclear magnetic resonance. Intensive research in the past several years has produced materials of extremely high purity with consequent advances in the understanding of their properties. Impurities can be introduced in known concentration and the resultant changes in electronic structure have been investigated by other means in previous studies. In this way one can control and vary the concentration of conduction electrons and paramagnetic impurities, a situation which makes nuclear resonance investigations exceedingly attractive. The electronic structures, intermediate in many respects between those of metals and insulators, should allow a variety of interactions between the nuclei and their lattice.

The nuclear magnetic resonances of dielectric substances have been extensively investigated and the lines observed are usually broadened by internuclear dipole-dipole interactions. Van Vleck[2] has shown that dipole-dipole broadening is a fundamental property of a crystal lattice and the effects are observed in metals as well as insulators. From Van Vleck's theory one can obtain lattice parameters in favorable instances. Pound[3] and Bloembergen[4] have shown quadrupole interactions

[1] H. S. Gutowsky, Ann. Rev. Phys. Chem. **5**, 333 (1953).

[2] J. H. Van Vleck, Phys. Rev. **74**, 1168 (1948).
[3] R. V. Pound, Phys. Rev. **79**, 685 (1950).
[4] N. Bloembergen, *Nuclear Magnetic Relaxation* (Martinus Nijhoff, The Hague, 1948).

to be a determining factor in the shape and width of nuclear magnetic resonances in some insulators. Multiplet structure in liquids has provided information on molecular configuration and chemical bonding.[5–7] This type of nuclear exchange interaction, first discussed by Ramsey and Purcell in covalent bonds, should also be effective in solids when the nuclei have large atomic numbers.

In metals the nuclei have been shown to interact with the conduction electrons, the neighboring nuclei, and to couple to the crystalline field gradients via nuclear quadrupole moments. Interactions with conduction electrons have been shown by Knight[8] to shift the nuclear resonance frequency from that observed in nonmetals. Korringa[9] has discussed spin-lattice relaxation in terms of this interaction and has related the frequency shift to relaxation times. Experiments by Gutowsky and McGarvey[10–12] have confirmed the conduction electron relaxation mechanism for several metals. Bloembergen and Rowland,[13] in a summary of nuclear resonance in metals, have shown the importance of electric quadrupole interactions as well as illustrating in detail some of the effects of conduction electrons.

Ruderman and Kittel[14] have recently proposed that internuclear exchange coupling[5] is important in metallic silver and they have derived the general theory for metals. This theory is applicable to other metals and the effect will be important when the atomic number is high. Bloembergen and Rowland[15] have employed this theory in their analysis of nuclear resonance experiments on metallic thallium. They have further derived the corresponding theory for insulators and applied this analysis to thallic oxide.

In the present paper we present the results of a nuclear magnetic resonance investigation of the semiconductors InSb and GaSb. Among other things it will be shown that the internuclear exchange interaction is dominant in determining the resonance widths and shapes in these compounds. Anderson[16] has extended the work of Ruderman and Kittel[14] and Bloembergen and Rowland[15] to the case of semiconductors. Fundamental information regarding the band structure of semiconductors is obtainable from the nuclear resonance measurements.

II. APPARATUS

The resonances were observed with a Pound-Knight-Watkins spectrometer.[17,18] The rf unit, 280 cycle modulation generator, and lock-in amplifier were built from Watkins' diagrams. The rf unit is powered by a Lambda Model 25 regulated power supply and a dc filament supply. Frequency measurements are made with a BC-221 frequency meter and the oscillator is monitored with a National HRO-60 communications receiver. Resonances are displayed on a Leeds and Northrup Speedomax recorder with a -5 to 0 to $+5$ millivolt range and a one-second pen. The lock-in amplifier is designed to allow observation with 2, 8, or 18 sec time constants. The 280 cycle sine-wave modulation is introduced by two coils taped to the magnet pole faces and is variable from 0–5 gauss peak-to-peak. The sample coil is mounted in a cryostat, designed by Dr. W. P. Slichter, similar to that described by Gutowsky *et al.*[19] Measurements at liquid nitrogen temperature were made by actually submerging the sample coil assembly in the nitrogen. The compensation coil, used to balance out 280-cycle pickup, consists of a double layer, three inches long, of No. 30 wire wound around the outside of the cryostat dewar.

A permanent magnet with a field of approximately 6520 gauss in a 2-inch gap 6 inches in diameter was used. The magnet was designed and constructed by the Indiana Steel Products Company, Valparaiso, Indiana, under the direction of Mr. H. L. Johnson. The design is similar to that of the magnet described by Gutowsky *et al.*[19] Proton resonances observed in water show that homogeneity at the center of the magnet gap is at least as good as 0.5 gauss over the 1-cc samples used. The field can be swept over a range of about 120 gauss by means of coils of 2000 turns of No. 20 wire around each Alnico pole. Current varying linearly in time is provided by an electronic regulator[19] and measured with a Sensitive Research Instrument Corporation Model C dc milliammeter. This meter, with ten overlapping ranges from 1.5 to 1500 ma full scale, is very useful for both high resolution and broad line measurements.

III. EXPERIMENTAL RESULTS

A. Gallium Antimonide

In gallium antimonide resonances of Ga^{69}, Ga^{71}, Sb^{121}, and Sb^{123} were observed. Table I lists pertinent data for the nuclei under consideration. These data are taken from the table published by Varian Associates. Two different samples of the highest purity obtainable

[5] N. F. Ramsey and E. M. Purcell, Phys. Rev. **85**, 143 (1952).
[6] Gutowsky, McCall, and Slichter, J. Chem. Phys. **21**, 279 (1953).
[7] N. F. Ramsey, Phys. Rev. **91**, 303 (1953).
[8] W. O. Knight, Phys. Rev. **76**, 1259 (1949).
[9] J. Korringa, Physica **16**, 601 (1950).
[10] H. S. Gutowsky and B. R. McGarvey, J. Chem. Phys. **20**, 1472 (1952).
[11] B. R. McGarvey and H. S. Gutowsky, J. Chem. Phys. **21**, 2114 (1953).
[12] H. S. Gutowsky, Phys. Rev. **83**, 1073 (1951).
[13] N. Bloembergen and T. J. Rowland, Acta Metallurgica **1**, 731 (1953).
[14] M. Ruderman and C. Kittel, Phys. Rev. **96**, 99 (1954).
[15] N. Bloembergen and T. J. Rowland, Office of Naval Research Technical Report 205, October 5, 1954 (unpublished). We are indebted to Dr. Bloembergen for kindly providing us with a copy of this report.
[16] P. W. Anderson (private communication).
[17] R. V. Pound and W. D. Knight, Rev. Sci. Instr. **21**, 219 (1950).
[18] George D. Watkins, thesis, Harvard University, 1952 (unpublished).
[19] Gutowsky, Meyer, and McClure, Rev. Sci. Instr. **24**, 644 (1953).

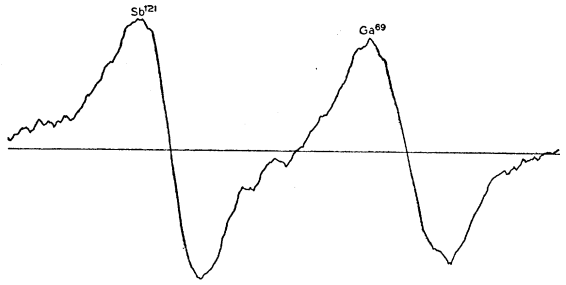

FIG. 1. Typical recorder traces of the derivative of the Ga^{69} and Sb^{121} resonances.

were used. These samples, as well as those of indium antimonide, were put at our disposal by Dr. H. J. Hrostowski, of these Laboratories, who also kindly supplied the analysis of donor and acceptor concentrations. Both GaSb samples were p-type with a hole concentration of about $10^{17}/cm^3$ at room temperature and at liquid nitrogen temperature. Because of the relatively high resistivity ($\sim$0.06 ohm cm), the skin depth at 8 Mc/sec was about 0.02 cm. Powder samples could easily be prepared and relatively large single crystals could be used with sufficient penetration of the radio-frequency energy. The sample used for most of the measurements was a powder prepared from a zone refined polycrystalline bar. In order to determine the orientation dependence of the resonance a single crystal with the $\langle 100 \rangle$ direction along the axis of the coil was used. Since results, except for signal to noise ratios, were the same for both the single crystal and the powder samples and were furthermore not temperature dependent between 77°K and 300°K, we report only the results on the powder at 77°K.

Typical recorder traces of the derivative of the Ga^{69} and Sb^{121} resonances are shown in Fig. 1. The lines were obtained by sweeping the magnetic field and the peak-to-peak widths are five to six gauss.

Although no very accurate measurements of the central frequency of these broad lines were possible, no shifts of the central frequencies from the values listed in the Varian Associates table were detected within an experimental accuracy of 2 kc/sec in 6–8 Mc/sec. Line shape measurements are presented in Table II. Column 2 lists the separation, in gauss, of the points of maximum deflection of the derivative curves plotted. The values quoted are the average of several determinations and limits of experimental error are presented.

The experimental absorption second moments of the lines are listed in column 3. These are average values from several traces and are calculated from the formula,[20]

$$\Delta H_2{}^2=(1/3)\int_{-\infty}^{\infty}(H-H_0)^3\left(\frac{dI}{dH}\right)dH\Big/\int_{-\infty}^{\infty}\times(H-H_0)\left(\frac{dI}{dH}\right)dH.$$

[20] G. E. Pake and E. M. Purcell, Phys. Rev. 74, 1184 (1948).

The precision of the second-moment determinations is not as good as that obtained for the line widths owing to the relative importance of the tails of the trace. Also errors in the second moments are introduced by base line drift and the difficulty in placing the line center. Close agreement between the average values for the two halves of the lines confirmed the visual evaluation that the lines are symmetrical. Even though the $Ga^{69}-Sb^{121}$ pair almost overlaps, the individual lines look fairly symmetrical and the second moments for the upper and lower frequency halves agree. However additional difficulty in selecting a base line was encountered and the data are not highly reliable.

In column 4, theoretical second moments calculated from Van Vleck's[2] equation for dipole-dipole broadening are given.

$$\Delta H_2{}^2=\left(\frac{3}{5}\right)I(I+1)\gamma^2\hbar^2\sum_j r_{0j}{}^{-6}+\left(\frac{4}{15}\right)\sum_f I_f(I_f+1)\gamma_f{}^2\hbar^2 r_{0f}{}^{-6}. \quad (1)$$

Lattice constants were taken from the *Handbook of Chemistry and Physics*.[21]

TABLE I. Pertinent nuclear data.

Nucleus	Frequency (mc/sec)	Field (gauss)	Spin	Quadrupole moment (10^{-24} cm^2)	% Abundance
Ga^{69}	6.67	6520	3/2	0.2318	60.2
Ga^{71}	8.47	6520	3/2	0.1461	39.8
In^{113}	6.06	6520	9/2	1.144	4.16
In^{115}	6.08	6520	9/2	1.161	95.84
Sb^{121}	6.64	6520	5/2	−1.3	57.25
Sb^{123}	3.60	6520	7/2	−1.7	42.75

The fifth column presents the experimental integrated intensities in the same arbitrary units used for the InSb intensities.[22] These are compared with the theoretical values in the last column. The permanent magnetic field was homogeneous to within $\pm\frac{1}{2}$ gauss and the modulation was kept small compared with the line width in order to eliminate modulation broadening.

[21] *Handbook of Chemistry and Physics* (Chemical Rubber Publishing Company, Cleveland, 1948), thirtieth edition.

[22] In these units D, the recorder deflection, is measured in volts by the calibrator, H is the magnetic field and γ the nuclear gyromagnetic ratio. In order to express the integrated intensity in terms of recorded quantities we integrate by parts.

$$\int_0^\infty I d\nu = I\nu\Big|_0^\infty - \int_0^\infty \nu dI.$$

For a reasonable line shape $I\nu|_0{}^\infty=0$ so

$$\int_0^\infty I d\nu = -\int_0^\infty \nu dI = -\gamma\int_0^\infty H dI = -\gamma\int_0^\infty H\left(\frac{dI}{dH}\right)dH.$$

Now $D=\left(\frac{dI}{dH}\right)\Delta H_m$ where ΔH_m is the modulation width. Therefore

$$\int_0^\infty I d\nu \propto \frac{\gamma}{\Delta H_m}\int_0^\infty H D dH.$$

Saturation effects were noticed in Ga^{71} and Ga^{69}, but not in Sb^{121}. Observations reported were all taken at the lowest possible oscillator power level. As the power level was increased saturation appeared in the Ga^{71} resonance before it was seen in the Ga^{69} while within the power limits available the Sb^{121} did not change.

B. Indium Antimonide

In indium antimonide resonances of Sb^{121} and In^{115} were observed. The In^{113} is only 4.16% abundant and was too weak to be detected. The Sb^{123} resonance was not seen, presumably because it was too weak and too broad. The In^{115} resonance on the other hand, had the largest signal-to-noise ratio of any of the lines observed in either of the two compounds.

The InSb samples used were purer than the GaSb samples. In GaSb, the density of impurities acting as acceptors was $\sim 10^{17}/cm^3$ and the total impurity concentration was at least this high. InSb had net acceptor impurity concentrations of $\sim 10^{15}/cm^3$ in the two samples studied most extensively. These samples were intrinsic conductors at room temperature containing

TABLE II. Resonance, widths, second moments, and intensities.

	Nucleus	δH (gauss)	Experimental ΔH_2^2 (gauss^2)	ΔH_2^2 (gauss^2) Calc. Eq. (1)	Theoretical intensity[a]	Experimental intensity
GaSb	Ga^{69}	5.1 ±0.14	6.5	1.20	0.020	0.024
	Ga^{71}	5.58±0.1	6.2±0.3	1.20	0.028	0.061
	Sb^{121}	4.7 ±0.1	6.7	1.05	0.045	0.024
	Sb^{123}	5.1 ±0.2	8.4±0.9	0.93	0.020	
InSb	In^{115}	9.0 ±0.2	24±1	1.65	0.167	0.167
	Sb^{121}	17.5 ±0.6	65±4	2.52	0.045	0.034

[a] Taken from the Varian N.M.R. Table, constant field. The experimental values are given in arbitrary units the In^{115} value being adjusted to the theoretical value.

$\sim 3\times 10^{16}/cm^3$ electrons and holes. At 77°K, the other operating temperature, they are extrinsic, p-type semiconductors with a mobile hole concentration of $\sim 3\times 10^{15}/cm^3$. Despite the change in carrier concentration by an order of magnitude between these two temperatures, no line shape changes were observed.

No differences were observed between the line shapes in a single crystal sample and a polycrystalline powder. The widths between extrema for the In^{115} resonance, $\delta H(In^{115})$, in the single crystal, were measured as a function of angle of orientation. The crystal was rotated in increments of 30° about an axis along the ⟨100⟩ direction which was also the coil axis. It was seen that $\delta H(In^{115})$ was equal to the powder value and independent of orientation. Both the In^{115} and Sb^{121} lines were Gaussian in shape. The In^{115} line for the powder sample at 77°K is shown in Fig. 2. The Gaussian shape function $C\exp[-K(H-H_0)^2]$ is plotted as crosses and fits the recorder trace quite well. The circles are a plot of the Lorentzian shape function $C/[1+(H-H_0)^2]$ for comparison. Both shape functions were made to pass through the center point and the maximum. Comparison is made for only one-half the line because of slight distortion of the other half by the In^{113} resonance.

Other experimental results are recorded in Table II. Owing to the great strength of the In^{115} its results are the most reproducible. The Sb^{121} resonance, on the other hand, was the weakest observed and its properties are not very accurately determined, particularly the second moment. No saturation effects were seen.

In addition, a single crystal of InSb was measured and then plastically deformed 20% by E. S. Greiner, of these Laboratories. The In^{115} resonance, observed before and after compression, showed a reduction in intensity by a factor of ~4.7. Although the In^{115} resonance was weak, there was no clear indication that it had been broadened or distorted. The 4.7 fold reduction represents the reduction of the peak derivative signal.

IV. DIPOLE-DIPOLE, QUADRUPOLE, AND T_1 EFFECTS

The most striking experimental results are the widths of the absorption lines. These line widths will be explained below by a nuclear spin exchange mechanism. Before this, however, it is necessary to examine several more traditional mechanisms which might determine the line widths and shapes. These are dipolar broadening and first and second order quadrupole interactions.

We see from Table II that the measured second moments are from five to 35 times larger than those calculated from Eq. (1). Since this relation is an exact expression for the contributions of dipolar broadening to the second moment we must look for additional mechanisms to explain the observations. Further evidence that dipolar broadening is not important in indium and gallium antimonides is furnished by the experiments on the orientation dependence of the line widths in single crystals. No change in width within experimental error was observed in the In^{115} resonance in InSb on rotation of the sample in 30° increments while the theoretical second moment calculated from Van Vleck's[2] Eq. (11) changes by a factor of 3.5.

All the nuclei observed have large electric quadrupole moments. Both InSb and GaSb have wurtzite struc-

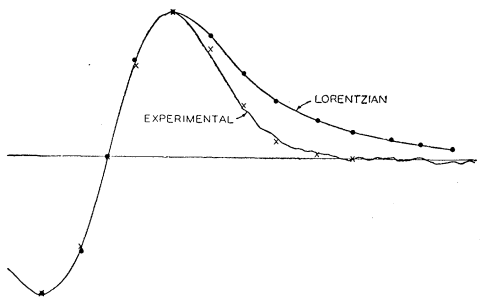

FIG. 2. Typical recorder trace of the derivative of the In^{115} resonance. Crosses are plotted from the Gaussian shape function and circles from the Lorentzian shape function.

tures where each atom is surrounded by four tetrahedral bonds to atoms of the other type. In a perfect crystal of this symmetry, there should be no electric field gradient at the nuclei. However, it is well known that actual crystals are not perfect and it has been demonstrated that even cubic crystals exhibit quadrupole interactions. Watkins and Pound[23] have shown that the integrated absorption intensities in KBr and KI are smaller than predicted by theory. They attribute this reduction to quadrupole splitting where random electric field gradients were established by lattice imperfections.

Pound[3] and Bersohn[24] have carried through perturbation theory treatments of quadrupole interactions in crystals. The resultant equation expresses the energy of the nuclear state as a power series in $(e^2Qq/\gamma\hbar H)$ where e is the proton charge, Q the nuclear quadrupole moment and q the electric field gradient at the nucleus. This fraction is small compared with unity in cases of interest in nuclear magnetic resonance and only the terms proportional to the first and second powers of $(e^2Qq/\gamma\hbar H)$, i.e., the first- and second-order terms, need be considered here. If the observed broadening is caused by the first-order terms then $(e^2Qq/\gamma\hbar H)$ is of the order of 10^{-3} and the second-order terms are negligible. The $m_I=\frac{1}{2}\leftrightarrow-\frac{1}{2}$ transitions are unaffected by first order quadrupole effects and therefore if the line shapes were the result of first-order broadening a sharp central spike would remain. The Gaussian shapes observed would require an extremely unlikely distribution of field gradients q. If the broadening were caused by the second-order quadrupole terms then $(e^2Qq/\gamma\hbar H)^2$ is of the order of 10^{-3} and the first-order splitting would be so great that only the $m_I=\frac{1}{2}\leftrightarrow-\frac{1}{2}$ transitions would be observable. As second-order quadrupole broadening results in unsymmetrical lines it is inconsistent with the present observations. Furthermore, the reduction in intensity of the In^{115} resonance in InSb after plastic deformation is proof that most of the components have not been split out in the undeformed crystal. We observe an intensity decrease by a factor of 4.7 in this case whereas a decrease by a factor of 6.6 would result if no quadrupole splitting was originally present and only the $m_I=\frac{1}{2}\leftrightarrow-\frac{1}{2}$ components remained after deformation. A further argument against the quadrupole broadening mechanism is provided by the relative line widths. For example, $Q(Ga^{69})/Q(Ga^{71})>1$, yet $\delta H(Ga^{69})/\delta H(Ga^{71})<1$.

Although quadrupole interactions are not responsible for line widths they do seem to account for the relaxation times observed. The relaxation time was measured by the onset of saturation in Ga^{69} to be $\sim$0.1 second. Saturation was first noticeable at lower power levels in Ga^{71} and corresponded to $T_1\sim0.2$ seconds. No tendencies of the Sb^{121} resonance to saturate could be observed indicating a shorter relaxation time. These values are roughly proportional to the quadrupole moments.

Finally it is probable that the deviation of relative intensities from the predicted values (see Table II) is due to quadrupole splitting, but not enough experimental evidence is available to corroborate this contention at this time.

V. PHYSICAL MODEL AND THEORY

Nuclear spin exchange via electron interactions was first described by Ramsey and Purcell[5] and applied to covalent bonds. Their theory has recently been modified and applied to metals by Ruderman and Kittel.[14] Regardless of the type of substance the basic mechanism is the hyperfine interaction of electron spin moments with nuclear spin moments. An electron in the vicinity of a nuclear spin moment μ_i will be polarized by that moment. The polarized electron then presents an effective field at another nucleus designated μ_j. By the same kind of hyperfine interaction μ_j feels the effect of the net polarization and in this fashion interacts with μ_i. It is apparent that for this effect to be large the electron must spend an appreciable time in the vicinity of both nuclei. Therefore we will be concerned with binding electrons only. The strength of this interaction will depend upon the magnitudes of μ_i and μ_j as well as upon other parameters which will be discussed in more detail below. It is possible to describe a polarization of electron spin states mathematically in terms of perturbation theory. The unperturbed, unpolarized electrons may be described by a wave function ψ_0 while the polarized case will correspond to mixing contributions from other states. The final function will represent the electron spin polarization by including wave functions in which the electron spins are aligned. Because of the large separation of electron energy states compared to thermal energy it is usually a good approximation to assume that all electronic states below a certain energy are filled while those above are empty. Furthermore, in the filled states it will be found that wave functions corresponding to both orientations of the electron spin are occupied by electrons. Therefore in perturbing the occupied states (where the electrons are found and hence the states which must be perturbed) we need only consider contributions from the unoccupied states. In solids, where one-electron wave functions are used, the exclusion principle does not influence the exchange either through the nuclear functions or the electronic functions but only through its determining influence upon the population of states. This follows from the fact that the Bloch functions for electrons in a solid are traveling waves and hence the interaction between μ_i and μ_j is essentially a double scattering process rather than an overlap of wave functions of electrons on each nucleus. This scattering is virtual rather than real because the linkage

[23] G. D. Watkins and R. V. Pound, Phys. Rev. **89**, 658 (1953).
[24] R. Bersohn, J. Chem. Phys. **20**, 1505 (1952).

involves a mixing of states which is a virtual excitation of electrons.

A quantitative expression for nuclear exchange interaction in semiconductors has been derived by Anderson[16] along the lines followed by Ruderman and Kittel[14] for metals. The highlights of Anderson's derivations are as follows. Assuming Bloch wave functions of the form $\varphi_k(\mathbf{r})=u_k(\mathbf{r})e^{i\mathbf{k}\cdot\mathbf{r}}$ and using Ramsey's perturbing Hamiltonian $\mathcal{H}_3$ the exchange interaction is

$$H_{ij}=-(\mathbf{S}\cdot\mathbf{I}_i)(\mathbf{S}\cdot\mathbf{I}_j)\Delta_i\Delta_j\sum_{k=0}^{\infty}\sum_{k'=0}^{\infty}\times\frac{\exp[-i(\mathbf{k}-\mathbf{k}')\cdot\mathbf{R}_{ij}]}{E_g+(\hbar^2\mathbf{k}'^2/2m_e)+(\hbar^2\mathbf{k}^2/2m_h)},\quad(2)$$

$$\Delta_i\equiv\int u_{k'i}\left[\frac{8\pi}{3}\mu_i\mu_e\delta(\mathbf{r}_i)\right]u_{ki}d\tau,$$

where i and j refer to nuclei i and j, S is electron spin, I is nuclear spin, Δ_i is the matrix element of hyperfine interaction for the s electrons with atomic wave functions $u_k(\mathbf{r})$, and E_g is the energy gap of the semiconductor. This expression can be integrated if spherical energy surfaces are assumed and the result is $\Delta E_{ij}=A_{ij}\mathbf{I}_i\cdot\mathbf{I}_j$, where

$$A_{ij}=\frac{3.36\times10^{-7}\Omega^2m^*\xi_i\xi_j\psi_i^2(0)\psi_j^2(0)\mu_i\mu_j}{I_iI_jR_{ij}^4}\ \text{sec}^{-1}\quad(3)$$

is the first and most important term in the solution. Here Ω=atomic volume, $m^*=4(m_e^*)^{\frac{3}{2}}(m_h^*)^{\frac{3}{2}}/(m_e^*+m_h^*)^2$, $\psi_i^2(0)$=the probability of finding the outer s electrons of atom i at its nucleus, and

$$\xi_i=\frac{[\psi_i^*(0)_{\text{hole}}\psi_i(0)_{\text{electron}}]_{\text{solid}}}{[\psi_i^2(0)]_{\text{atom}}},$$

$$R_{ij}=|\mathbf{r}_i-\mathbf{r}_j|.$$

It is important to remember that this perturbation applies only to s electrons. It is assumed that the hyperfine interactions of p, d, etc. electrons are negligible compared to that of s electrons. Furthermore, it is important to note that the nuclear exchange calculated here only results in line broadening when the interaction is between unlike nuclei.

One interesting point about the integration over the energy surfaces is that the solution does not include the energy gap E_g in the dominant term. It does enter into the higher order terms but these are negligible for near-neighbor interactions. The reason for this is that the high momentum states have the greatest statistical weight and compared to their energy separations E_g can be ignored. For R_{ij} large compared to near-neighbor separations the high momentum states lose their phase coherence and no longer add constructively, but for small values of R_{ij} they do and are the important terms.

The limiting accuracy of the calculation is the integration over momentum space in both the valence and conduction bands. This integration will be discussed below in conjunction with an attempt to determine the absolute value of A_{ij}.

VI. LINE SHAPES

The shapes of the resonance lines will be calculated assuming the interaction discussed in the last section. Van Vleck has presented expressions for the second moments and fourth moments to be expected from exchange broadening. However, his expression for the fourth moments is difficult to evaluate and we have determined the theoretical line shapes not by comparing second and fourth moments but by numerically considering only nearest-neighbor interactions. We consider three interacting nuclear species, i, j, and k (e.g., In^{115}, Sb^{121}, and Sb^{123} respectively in InSb) and assume the resonance of nucleus i is to be observed. By a slight extension of the arguments presented by Gutowsky, McCall, and Slichter[6] the resonance of i is seen to occur at

$$\omega_i=\gamma_i[H_i+(C_{ij}\gamma_jM_j/h)+(C_{ki}\gamma_kM_k/h)],\quad(4)$$

where M_j and M_k are quantum numbers[25] for the spin groups of nuclei j and k and $C_{ij}\gamma_i\gamma_j\equiv A_{ij}$. The components thus occur at an equivalent magnetic field given by the bracketed term in Eq. (4). The constants C_{ij} and C_{ki} depend on the electronic properties of the same elements so they are equal, $C_{ij}=C_{ki}=C$. If K is written for γ_k/γ_j Eq. (4) becomes

$$\omega_i=\gamma_i[H_i+(C\gamma_j/h)(M_j+KM_k)].\quad(5)$$

With this equation the line shape may be calculated by computing the positions and intensities of the components and taking a suitable envelope of the resulting spectrum. The intensities are obtained in arbitrary units, depending only upon the relative weights of the spin states corresponding to M_j and M_k. The broadening is obtained in terms of the constant C which may then be found by comparison of the calculated and experimental curves. Line shapes for all of the resonances observed in InSb and GaSb have been calculated in the foregoing manner and are all Gaussian, in agreement with the experimental results. This Gaussian shape is to be expected considering the large numbers of nuclear spin orientations allowed. In the In^{115} Sb resonance, for example, there are 475 random components from nearest neighbor interactions alone.

VII. RELATIVE LINE WIDTHS

Following the procedure of Sec. VI one may obtain the resonance widths as a function of the field parameter $(C_{ij}\gamma_j/\hbar)$ by directly plotting the line shape. Therefore

[25] Let there be n_j nuclei in spin group j. Then if $F_j=n_jI_j$ we have $M_j=F_j, F_j-1, \cdots, -F_j$.

the relative line width may be obtained directly as the constant C_{ij} in any one compound cancels and γ_i and γ_j are known. This procedure assumes that only nearest neighbor interactions are appreciable as was previously justified through the rapid attenuation of A_{ij} with internuclear separation R_{ij}. Line width ratios have been computed in this way for InSb and GaSb and the results agree well with the experimental values.

A much simpler procedure, which allows the inclusion of second nearest neighbors, makes use of Van Vleck's equation (28).[2] Again the absolute value of A_{ij} is not required to determine the relative line widths, but we must use the radial dependence of A_{ij} which was shown (in Sec. V) to be an inverse fourth power. It will be shown in the following calculations that the line width contributions from second nearest neighbors are negligible in all the resonances reported here except for Sb in GaSb.

Van Vleck's equation (28) states

$$h^2\langle\Delta\nu_i^2\rangle_{Av}=\tfrac{1}{3}\textstyle\sum_f[I_f(I_f+1)\sum_j A_{ij}^2(R_{ij})], \qquad (6)$$

where the subscripts f refer to different nuclear species and the dipole-dipole terms have been omitted. Note that the dependence of A_{ij} on R_{ij} must be included. No interaction between like nuclei appears.

The comparison of relative line widths calculated by Eq. (6) and the experimental values is presented in Table III. The first column lists not the ratio of experimental line widths as measured but the values after correcting for dipolar broadening. The procedure followed was based upon the observed Gaussian line shapes. Since the peak-to-peak absorption derivatives were measured more precisely than the second moments these widths were converted to second moments by the relation $(1/4)\delta H^2=\Delta H_2^2$. Values of the second moment predicted from dipolar broadening were then subtracted from these experimental second moments and the results converted back to peak-to-peak absorption widths. The second column lists the theoretical ratios considering first and second nearest neighbors while the third column presents the effects of first nearest neighbors only. It can be seen that the antimony second nearest neighbors in GaSb have an appreciable effect. The $Sb^{121}-Sb^{123}$ exchange in these substances, while decreased compared to the GaSb exchange because of the larger separation, is increased, first by the larger number of second nearest neighbors (twelve), and second by a larger value of $\psi^2(0)$ for Sb compared to Ga. The values of $\psi^2(0)$ used will be discussed in the next section.

TABLE III. Relative line widths.

Nuclear ratio		Experimental width ratio, corrected	Theoretical ratio 1st and 2nd neighbor	Theoretical ratio 1st neighbor only
GaSb	$\frac{Ga^{71}}{Ga^{69}}$	1.11	1.00	1.00
	$\frac{Sb^{123}}{Sb^{121}}$	1.12	1.12	1.00
	$\frac{Ga^{71}}{Sb^{123}}$	1.08	0.99	1.21
InSb	$\frac{Sb^{121}}{In^{115}}$	2.00	1.73	1.73

VIII. ABSOLUTE VALUE OF A_{ij}

The energy surfaces in these compounds have previously been investigated in limited regions. Optical and Hall measurements of InSb[26] and GaSb[27] have been interpreted to yield values of the effective mass for holes and electrons. These measurements were made on electrons and holes occupying the bottom of the conduction band and the top of the valence band respectively. They indicate spherical energy surfaces in these regions. Values of the effective masses are listed in Table IV. However, the important contributions to the nuclear exchange come from the high momentum states in both bands, regions about which the experiments mentioned above tell us nothing.

TABLE IV. Effective masses of carriers in InSb and GaSb near the forbidden gap.

	m_e^*	m_h^*
InSb	0.025[a]	0.15[a]
GaSb	0.2[b]	0.4[b]

[a] H. J. Hrostowski (unpublished); more recent results indicate slightly different values.
[b] H. Leifer and W. C. Dunlap, Phys. Rev. **95**, 51 (1954).

The band structure of these compounds can be considered as arising from perturbations of the atomic functions. Isolated gallium, indium or antimony atoms have eight eigenstates in their outer shells. When compounds are formed the bonding orbitals are sp^3. There are four degenerate sp^3 bonding orbitals, and four degenerate sp^3 nonbonding orbitals. The former are the basis for the valence bands in the solid and the latter go into the first conduction band. In the solid the bonding and nonbonding orbitals are each split into four bands by interatomic interactions. The extent to which these bands are separated, and the shapes of the bands, are not known although calculations similar to those made for silicon and germanium[28] presumably could supply a great deal of information about the band structure. The magnitude of the interaction constant represents an experimental result which must be consistent with any calculation of the energy band surfaces. To show that the experimental results can be

[26] H. J. Hrostowski (private communication).
[27] H. Leifer and W. C. Dunlap, Phys. Rev. **95**, 51 (1954).
[28] F. Herman, Phys. Rev. **93**, 1214 (1954).

obtained with reasonable assumptions, consider two unlikely extremes. First we consider the minimum splitting case where the small measured values of effective mass are assumed to prevail throughout the entire band and where only one nondegenerate band lies low enough in energy to contribute appreciably. This corresponds to the electrons having only one quarter s character and the high momentum states in both valence and conduction bands possessing very large energies which increase the denominator of Eq. (2). The results of this approximation are listed in the first column of Table V and are seen to be smaller than the experimental values of 9.0 gauss for InSb and 5.6 gauss for GaSb. In order to calculate an extreme upper limit for the magnitude of A_{ij} we assume that the bands are degenerate everywhere, i.e., all four bands contribute equally, the effective masses equal the free electron mass, and that each atom is surrounded by four electrons with contributions from an s state and three p states, the latter being neglected. These values are listed in the last column. It is seen that the exchange interaction is quite sensitive to the energy surfaces while the measured values are reasonably located between the two extremes.

C. Herring has mentioned to the authors that in these lattices the "empty lattice" approximation should represent a reasonable description of the carriers over a major portion of the energy bands. By assuming that each electron and hole has the free electron mass, one quarter s character, and values of $\xi_i=\xi_j=0.74$ for InSb and $\xi_i=\xi_j=0.88$ for GaSb, agreement of Eq. (3) with the experimental line widths is obtained, showing the reasonable nature of this assumption.

It is an interesting coincidence that Eq. (11) of reference 14 gives exactly the same value of A_{ij} for InSb as our Eq. (3).

It is necessary to know the values of $\psi^2(0)$ for s-electrons in atomic gallium, indium and antimony. For gallium and indium measurements of hyperfine splitting by the $4s$ and $5s$ electrons in the doubly ionized state are available.[29] By comparing these values with those observed for the $4s$ and $5s$ electrons in copper and silver,[29] compromise values of $\psi_{Ga}{}^2(0)=8\times10^{25}$ cm^{-3} and $\psi_{In}{}^2(0)=16\times10^{25}$ cm^{-3} were used. Since no direct measurements had been made on Sb^{+4} the Fermi-Segrè formula was used in conjunction with a comparison with $\psi_{In}{}^2(0)$ and the value 24×10^{25} cm^{-3} appeared and was used for $\psi_{Sb}{}^2(0)$.

The exchange interaction between two nonidentical nuclei has been calculated from second-order perturbation theory. In the calculation it has been assumed that the exchange interaction is much smaller than the differences in resonance frequencies or that $A_{ij}\ll[|\gamma_i|-|\gamma_j|]H_0$. For the $Ga^{69}-Sb^{121}$ pair in GaSb at 6520 gauss this condition is just satisfied since the experimental value of $A_{ij}=0.8$ gauss while the measured value of the separation is 18.0 gauss. By varying the magnetic field strength it should be possible to change the separation and see how the lines collapse into a single line at small values of H_0, as predicted by Anderson.[30] It is planned to do this in the future.

TABLE V. Comparison of experimental and theoretical interaction constants.

	Minimum splitting case assuming	Experimental	Maximum splitting case assuming
	(1) m^* InSb $=0.03m$ m^* GaSb $=0.254m$		(1) m^* InSb $=m^*$ GaSb $=1$
	(2) Only one band contributes to each integration over k space of $\xi_i=\xi_j=\frac{1}{4}$		(2) Four bands contribute equally to each integration over k space or $\xi_i=\xi_j=1$
$\delta H_{\frac{1}{2}}$ $In^{115}Sb$ (gauss)	0.5	9.0	260
$\delta H_{\frac{1}{2}}$ $Ga^{71}Sb$ (gauss)	1.8	5.6	115

CONCLUSIONS

The nuclear magnetic resonances in InSb and GaSb have been observed and the following conclusions reached.

(1) Line widths and shapes are almost completely determined by a nuclear exchange mechanism involving electron spins.

(2) The magnitude of the exchange interaction depends upon the electron energy surfaces in valence and conduction bands with the largest contributions coming from states far from the Fermi level. Therefore the experimental interaction constants provide information about these relatively inaccessible regions of the energy bands.

ACKNOWLEDGMENTS

It is a pleasure to thank P. W. Anderson not only for the use of his calculations but also for many stimulating and informative discussions. N. Bloembergen first suggested the appropriateness of an exchange interaction. H. J. Hrostowski kindly provided the high quality samples used in this work.

J. M. M. wishes to thank H. S. Gutowsky for much good advice regarding building of the apparatus. He is also indebted to many colleagues at Bell Telephone Laboratories, particularly F. E. Radcliffe for advice in electronic matters and C. R. Geith for his excellent mechanical design and construction.

[29] Landolt-Börnstein, *Physikalisch-Chemische Tabellen* (Springer-Verlag, Berlin, 1952), Vol. 1, Part 5, pp. 19, 29.

[30] P. W. Anderson, J. Phys. Soc. Japan **9**, 316 (1954).